

A Study of C–F···M⁺ Interaction: Metal Complexes of Fluorine-Containing Cage Compounds

Hiroyuki Takemura,^{*,†} Sachiko Nakashima,[‡] Noriyoshi Kon,[‡] Mikio Yasutake,[§] Teruo Shinmyozu,[§] and Takahiko Inazu[‡]

Contribution from the Department of Chemistry, Faculty of Science, Kyushu University, Ropponmatsu 4-2-1, Chuo-ku, Fukuoka, 810-8560 Japan, Department of Chemistry, Faculty of Science, Kyushu University, Hakozaki 6-10-1, Higashi-ku, Fukuoka, 812-8581 Japan, and Institute for Fundamental Research of Organic Chemistry, Kyushu University, Hakozaki 6-10-1, Higashi-ku, Fukuoka, 812-8581 Japan

Received December 27, 2000. Revised Manuscript Received April 10, 2001

Abstract: The C–F···M⁺ interaction was investigated by observation of the NMR spectroscopic changes and complexation studies between metal cations and the cage compounds **1** and **2** which have fluorobenzene units as donor atoms. As a result, the interaction was detected with all of the metal cations which form complexes with **1** and **2**. The stability of the complexes of **1** and **2** was determined by the properties of the metal cations (ionic radii and degree of hydrolysis), not by the hard–soft nature of the cations. Crystallographic analyses of Tl⁺ ⊂ **1** and La³⁺ ⊂ **2** provided structural information (interatomic distances and bond angles), and the bond strengths, C–F···M⁺, O···M⁺, and N···M⁺, were estimated by Brown's equation based on the structural data. Short C–F···Tl⁺ (2.952–3.048 Å) distances were observed in the complex Tl⁺ ⊂ **1**. The C–F bond lengths in the complexes, Tl⁺ ⊂ **1** and La³⁺ ⊂ **2**, are elongated compared to those of the metal-free compounds. Interestingly, no solvent molecules including water molecules were coordinated to La³⁺ in the La³⁺ ⊂ **2**. The stabilization energy of cation–dipole interaction was calculated on the basis of the data from X-ray crystallographic analysis, and it is roughly consistent with the –Δ*H* values estimated in solution. Thus, the C–F···M⁺ interaction can be expressed by the cation–dipole interaction. This result explains the fact that compound **1** which has fluorine atom as hard donor strongly binds soft metals such as Ag⁺ and Tl⁺. Furthermore, it was concluded that the fluorobenzene unit has a poor electron-donating ability compared to that of ether oxygen or amine nitrogen, and thus the ratio of the coordination bond in C–F···M⁺ is small. The specific and remarkable changes in the ¹H, ¹³C, and ¹⁹F NMR spectra were observed accompanied by the complexation between M⁺ and the hosts **1** and **2**. These spectral features are important tools for the investigation of the C–F···M⁺ interaction. Furthermore, F···Tl⁺ spin couplings were observed at room temperature in the Tl⁺ ⊂ **1**, **2** (*J*_{F–Tl} = 2914 Hz for Tl⁺ ⊂ **1** and 4558 Hz for Tl⁺ ⊂ **2**), and these are clear and definitive evidence of the interaction.

Introduction

Glyme, ethers, and amines are frequently used in organic synthesis as good solvation reagents for metal or metal cations. It is well-known that intramolecular oxygen or nitrogen interacts with organometallic reagents and greatly affects the regio- and stereoselectivity. These phenomena result from the fact that oxygen and nitrogen have large electronegativities and adequate ionization potentials and interact with metal cations attractively. The driving forces of the high cation affinities of crown ethers, macropolycyclic amines, and cryptands are based on this nature. On the other hand, it has become apparent that halocarbons, C–X (X = F, Cl, Br, I), which have highly electronegative halogen atoms, interact with cations according to recent research studies.¹ Despite the remarkable progress in fluorine chemistry,

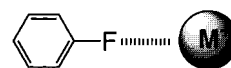


Figure 1.

the C–F unit in which the most electronegative element is covalently bonded to a carbon atom has not received much attention as a cation donor like oxygen (C–O) or nitrogen (C–N). On the other hand, crystallographic studies revealed that various metal complexes show short C–F···M⁺ distances, and the interaction is predicted on the basis of these short interatomic distances. However, the study of the interaction in solution is still in an early stage (Figure 1).²

We showed that a macrocyclic cage compound system which has fluorine atoms in its cavity is ideal to investigate the C–F···M⁺ interaction because the system is not affected by external conditions such as the effect of solvents. Compound **1**, constructed from six fluorobenzene units, is a unique example that captures metal cations only by fluorine atoms (Figure 2).³

(2) Plenio, H. *Chem. Rev.* **1997**, *97*, 3363–3384 and references therein.

(3) Takemura, H.; Kon, N.; Yasutake, M.; Kariyazono, H.; Shinmyozu, T.; Inazu, T. *Angew. Chem.* **1999**, *111*, 1012–1014; *Angew. Chem., Int. Ed.* **1999**, *38*, 959–961.

[†] Department of Chemistry, Faculty of Science, Kyushu University, Ropponmatsu 4-2-1, Chuo-ku, Fukuoka, 810-8560 Japan.

[‡] Department of Chemistry, Faculty of Science, Kyushu University, Hakozaki 6-10-1, Higashi-ku, Fukuoka 812-8581 Japan.

[§] Institute for Fundamental Research of Organic Chemistry, Kyushu University, Hakozaki 6-10-1, Higashi-ku, Fukuoka, 812-8581 Japan.

(1) (a) Kulawiec, R. J.; Crabtree, R. H. *Coord. Chem. Rev.* **1990**, *99*, 89–115. (b) Murray-Rust, P.; Stallings, W. C.; Monti, C. T.; Preston, R. K.; Glusker, J. P. *J. Am. Chem. Soc.* **1983**, *105*, 3206–3214.

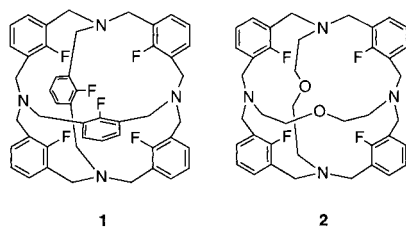


Figure 2. Structures of **1** and **2**.

We have investigated the C–F···M⁺ interaction between cage compound **1** and alkali metal cations, ammonium, and silver ion by complexation measurements, NMR spectra, and isolation of the complexes. As a result, some specific features, that is, remarkable changes in the ¹H, ¹³C, and ¹⁹F NMR spectra, short C–F···M⁺ distances and elongation of C–F bonds in the crystal structure of the complexes were observed when the interaction occurred. At the same time, we reported that the spatial arrangement and number of the C–F units are very important to capture the cations and observe the C–F···M⁺ interaction with sufficient strength. Among several fluorine-containing macrocyclic compounds, compound **1** is the most suitable compound for this purpose.⁴ Then, we had to estimate the quantitative data for the interaction, and this was achieved by the measurements of thermodynamic parameters of the cation inclusion process between alkali cations and **1**. As a result, the reaction gave relatively large $-\Delta H$ values (~ -16.1 kcal mol⁻¹).⁵ The values indicate that the interaction stabilizes the cations to an extent similar to that of crown ethers or cryptands in some cases (solvents in the measurements are different), and thus, the C–F···M⁺ interaction was considered to be comparable to that of ether oxygen.

In the next step, we must answer the following questions: (1) Does the interaction function with any kind of cations? (2) Are there any selectivities or differences in affinities among metal cations? To clarify these areas, we investigated the reaction between several metal cations and host compounds **1** and **2**. Because new host molecule **2** has fluorine, oxygen, and nitrogen atoms as donors, we can estimate the contribution of each ligand to the stabilization of the cations simultaneously.

Results and Discussion

Interaction with Metal Cations. The presence of C–F···M⁺ interaction can be qualitatively estimated by NMR spectra, and thus the interaction between NMR-observable metal cations and **1** and **2** was investigated.^{2–5} The complexation study showed that metal cations can be classified into three groups as follows. In the first group, they form stable complexes (I), in the second group, the complexation is observable by NMR spectra (II), and in the third group, they are hydrolyzed and form protonated species, $n\text{H}^+ \subset \mathbf{1}, \mathbf{2}$ (III). The experiments were carried out by mixing metal triflates and **1** or **2** in a mixed solvent CDCl₃/CD₃CN (= 1/1, v/v), and the ¹H, ¹⁹F NMR changes were monitored. The mixed solvent was chosen by considering the solubility of the hosts and metal salts. The reactions proceeded very slowly, and more than 3 days at 60 °C were needed until the reactions had equilibrated. Some metal salts were hydrolyzed by small quantities of water in the experimental conditions and released protons, which formed

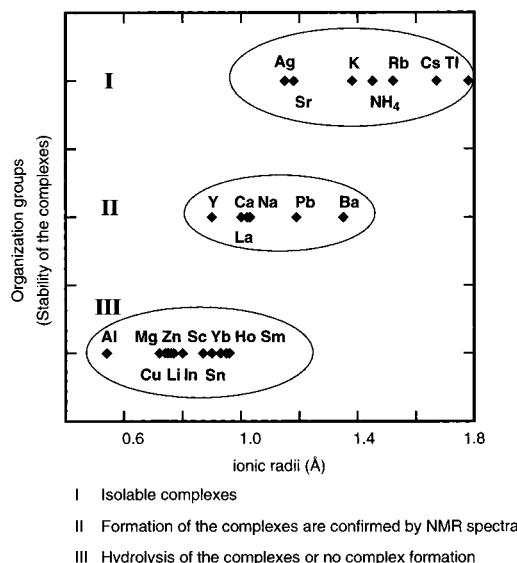


Figure 3. The relationship between the stability of the complexes and the ionic radii.

protonated species, $n\text{H}^+ \subset \mathbf{1}, \mathbf{2}$. For example, the reaction between **1** and Sc(CF₃SO₃)₃ afforded $3\text{H}^+ \subset \mathbf{1}$ as colorless granules. Similarly, the reaction between **2** and La(CF₃SO₃)₃ gave a mixture of $2\text{H}^+ \subset \mathbf{2}$ and $\text{La}^{3+} \subset \mathbf{2}$.⁶ In this experiment, K⁺, Rb⁺, Cs⁺, Sr²⁺, Ag⁺, Tl⁺, and NH₄⁺ were classified into group I, Na⁺, Ca²⁺, Ba²⁺, Pb²⁺, Y³⁺, and La³⁺ were classified into group II, and Li⁺, Cu⁺, Mg²⁺, Zn²⁺, Sn²⁺, Al³⁺, In³⁺, Sc³⁺, Yb³⁺, Sm³⁺, and Ho³⁺ were classified into group III.⁷ As previously described, the complex formation of compound **1** is sensitive to the size of the cations, which was elucidated by measurements of the stability constants of the alkali metal complexes.⁵ Also in the experiment, small cations did not seem to form stable complexes. Here, we can create a diagram which shows the relationship between ionic radii and stability of the complexes (Figure 3). Obviously, groups I, II, and III can be correlated to ionic radii, and cations smaller than 1 Å do not form stable complexes with **1** and **2**. Furthermore, the stability is correlated to the hydrolysis constants *K* of the metal cations (Figure 4).⁸ Plots of the $-\log K$ and ionic radii show that metal cations which are hard to hydrolyze form stable complexes. Because the host molecules are basic, protonation occurs in preference to complexation when the metal cations are easily hydrolyzed. Furthermore, the C–F unit forms stable complexes with soft cations, Ag⁺ or Tl⁺, despite the hard nature of the fluorine atoms. Thus, the stability of the metal complexes is not related to the soft–hard combination of the donor–acceptor. Figure 4 is superimposable in Figure 3, and all three groups agree well; thus, the stability of the complexes is determined by the ionic radii and hydrolytic property of the metal cations.

(6) The component of $3\text{H}^+ \subset \mathbf{1}$ was determined by elemental analysis, and that of $2\text{H}^+ \subset \mathbf{2}$ was determined by X-ray crystallographic analysis. By NMR titration experiments using picric acid (1–4 mol equiv), $\text{H}^+ \subset \mathbf{1}$, $2\text{H}^+ \subset \mathbf{1}$, and $3\text{H}^+ \subset \mathbf{1}$ were clearly observed and distinguished by the ¹⁹F NMR spectra.

(7) By considering the ionic radii, Ag and Sr seem to be in Group II, and Ba seems to be in Group I. However, the host forms a stable complex with Ag which can be isolated, and complexation experiments with Ca, Sr, and Ba showed that complex formations are weak in the case of Ca and Ba, but it is strong in the case of Sr. The same phenomena were also observed in the case of host **2**. Furthermore, the host is protonated by the reaction with the salts of Ca, Sr, and Ba. Therefore, the experiments were carried out under basic conditions in the presence of small amounts of the hydroxides. Despite the large hydrolysis constants ($-\log K$) of Ca, Sr, and Ba (almost equal to alkali metal cations), the reaction between these salts and the host gave protonated species.

(8) Barnum, D. W. *Inorg. Chem.* **1983**, *22*, 2297–2305.

(4) Takemura, H.; Kariyazono, H.; Yasutake, M.; Kon, N.; Tani, K.; Sako, K.; Shinmyozu, T.; Inazu, T. *Eur. J. Org. Chem.* **2000**, 141–148.

(5) Takemura, H.; Kon, N.; Yasutake, M.; Nakashima, S.; Shinmyozu, T.; Inazu, T. *Chem. Eur. J.* **2000**, *6*, 2334–2337.

(6) Takemura, H.; Nakashima, S.; Kon, N.; Inazu, T. *Tetrahedron Lett.* **2000**, *41*, 6105–6109.

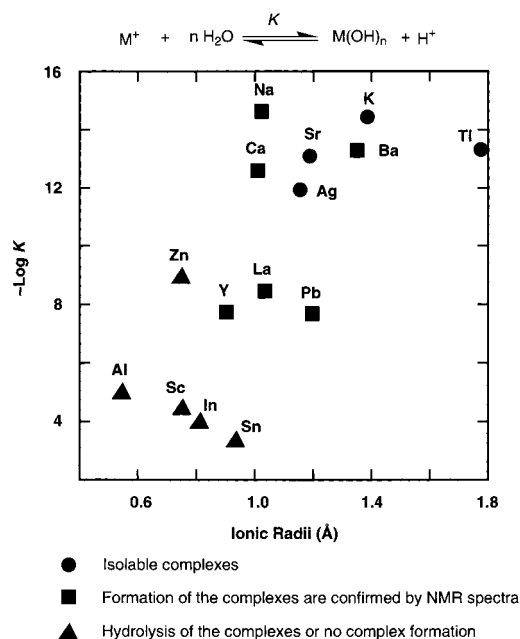


Figure 4. Plots of $-\log K$ vs ionic radii.

Therefore, we can speculate that any kind of metal cation interacts with the C–F unit (the reasons described below support this speculation). However, the hosts **1** and **2** are not adequate for investigating the interaction with small and easily hydrolyzable cations. For this purpose, we have to design another kind of host molecule which has a small cavity and does not contain nitrogen atoms.

Crystallographic Analyses and Brown's Equation. The X-ray crystallographic analysis elucidates structural information (interatomic distances and angles) of the C–F···cation system and particularly, the bond strengths of C–F···M⁺, O···M⁺, and N···M⁺, which can be estimated as numerical values using Brown's equation.⁹

The result of the crystallographic analysis of $\text{Ti}^+ \subset \mathbf{1}$ shows two kinds of structures each with 50% probability. One of them has a hexacoordinated structure, and another has a pentacoordinated structure with disordered C–F carbon atoms. However, we will discuss the hexacoordinated structure because the pentacoordinated structure has abnormal C–F bond lengths (Figure 5). The $\text{Ti}^+ \cdots \text{F}$ distances are 2.952–3.048 Å and are shorter than the sum of the van der Waals radii of the fluorine atom and the ionic radius of Ti^+ (3.25 Å). On the other hand, the $\text{Ti}^+ \cdots \text{N}$ distances are 3.470–3.652 Å and are longer than the sum of the van der Waals radii of the nitrogen atom and the ionic radius of Ti^+ (3.33 Å) (Table 1). Therefore, binding of a Ti^+ ion resulted from the interaction with fluorine atoms and that with nitrogen atoms is weak. Furthermore, an average C–F bond length is 1.364 Å, and this is longer than that of metal-free **1** (1.348 Å). This result is unequivocal evidence of the attractive interaction between C–F and Ti^+ . Every complex which we observed and reported ($\text{K}^+ \subset \mathbf{1}$, $\text{K}^+ \subset \mathbf{2}$, $\text{NH}_4^+ \subset \mathbf{1}$, $\text{Cs}^+ \subset \mathbf{2}$, $\text{Ti}^+ \subset \mathbf{1}$, and $\text{La}^{3+} \subset \mathbf{2}$) have elongated C–F bonds compared to those of the metal-free compounds.^{3,4,10}

The complex $\text{La}^{3+} \subset \mathbf{2} \cdot (\text{CF}_3\text{SO}_3^-)_3$ was obtained by the reaction between **2** and $\text{La}(\text{CF}_3\text{SO}_3)_3$ in $\text{CDCl}_3/\text{CD}_3\text{CN}$ (= 1/1,

(9) (a) Brown, I. D.; Altermatt, D. *Acta Crystallogr.* **1985**, *B41*, 244–247. (b) Altermatt, D.; Brown, I. D. *Acta Crystallogr.* **1985**, *B41*, 240–244.

(10) Recently, we succeeded the crystallographic analysis of the complexes, $\text{K}^+ \subset \mathbf{2}$ and $\text{Cs}^+ \subset \mathbf{2}$. Also in these cases, the C–F bonds are longer (1.382 and 1.369 Å on average, respectively) than that of metal-free compound (1.356 Å on average). See ref 14.

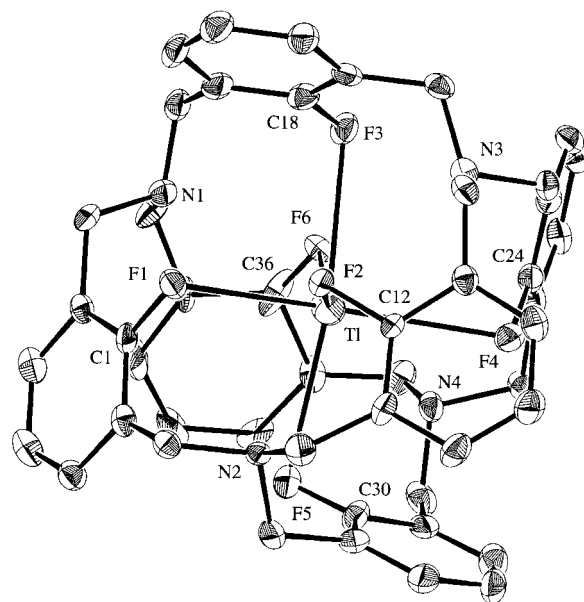


Figure 5. X-ray crystallographic structure of $\text{Ti}^+ \subset \mathbf{1}$ (H atoms are omitted for clarity).

Table 1. Representative Bond Lengths, Interatomic Distances (Å) and Bond Angles (deg) of $\text{Ti}^+ \subset \mathbf{1}$

bond lengths (Å)	interatomic distances (Å)	bond angles (deg)
C1–F1 1.359(10)	$\text{Ti}^+ \cdots \text{F1}$ 2.952(5)	C1–F1···Ti 96.6(4)
C12–F2 1.390(9)	$\text{Ti}^+ \cdots \text{F2}$ 2.995(5)	C12–F2···Ti 97.9(4)
C18–F3 1.35(1)	$\text{Ti}^+ \cdots \text{F3}$ 3.032(5)	C18–F3···Ti 96.9(4)
C24–F4 1.360(10)	$\text{Ti}^+ \cdots \text{F4}$ 2.984(5)	C24–F4···Ti 98.0(4)
C30–F5 1.36(1)	$\text{Ti}^+ \cdots \text{F5}$ 3.048(5)	C30–F5···Ti 93.7(5)
	$\text{Ti}^+ \cdots \text{N1}$ 3.539(7)	
	$\text{Ti}^+ \cdots \text{N2}$ 3.470(7)	
	$\text{Ti}^+ \cdots \text{N3}$ 3.509(7)	
	$\text{Ti}^+ \cdots \text{N4}$ 3.652(7)	

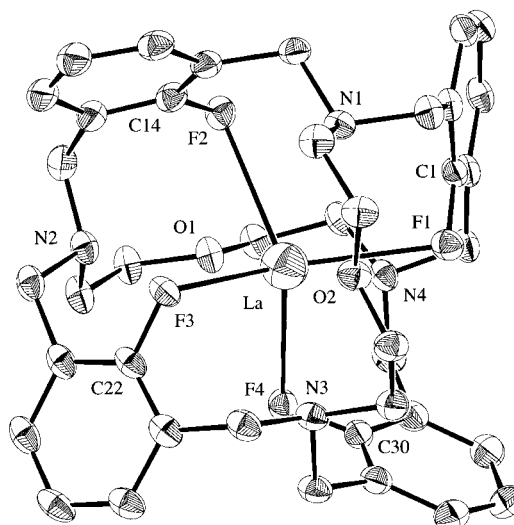


Figure 6. X-ray crystallographic structure of $\text{La}^{3+} \subset \mathbf{2}$ (H atoms are omitted for clarity).

v/v) as a mixture of $2\text{H}^+ \subset \mathbf{2}$ and the complex. Each structure of $\text{La}^{3+} \subset \mathbf{2}$ and $2\text{H}^+ \subset \mathbf{2}$ was clarified by X-ray crystallographic analysis, and Figure 6 shows the structure of $\text{La}^{3+} \subset \mathbf{2}$. Because La^{3+} is small (1.03 Å), the C–F···La distances (2.723–2.885 Å) become larger than the sum of the ionic radius of La^{3+} and the van der Waals radius of the fluorine atom (2.50 Å). However, also in this case, the C–F bond lengths (1.361–

Table 2. Representative Bond Lengths, Interatomic Distances (Å) and Bond Angles (deg) of La³⁺ **2**

	bond lengths (Å)	interatomic distances (Å)	bond angles (deg)
C1–F1	1.366(5)	La···F1 2.758(4)	C1–F1···La 100.3(2)
C14–F2	1.361(6)	La···F2 2.885(4)	C14–F2···La 100.9(2)
C22–F3	1.363(4)	La···F3 2.723(5)	C22–F3···La 107.1(3)
C30–F4	1.367(6)	La···F4 2.799(3)	C30–F4···La 104.2(2)
		La···N1 3.202(3)	
		La···N2 3.462(5)	
		La···N3 3.063(5)	
		La···N4 3.321(6)	
		La···O1 3.138(4)	
		La···O2 3.230(4)	

Table 3. Brown's Bond-valence, *s*, of the Complexes

	K ⁺ 1	Tl ⁺ 1	K ⁺ 2	Cs ⁺ 2	La ³⁺ 2
Σ _s (F···M)	0.834	0.318	0.620	0.689	0.682
Σ _s (O···M)	—	—	0.178	0.329	0.149
Σ _s (N···M)	0.164	0.087	0.212	0.395	0.314
V = ΣΣ _{s_x}	0.999	0.405	1.01	1.413	1.145

1.367 Å) are longer than those of the metal-free compound (1.355–1.358 Å) as shown in Table 2.

On the basis of the data from the crystallographic analysis, the bond strength between the cation and each ligand (F, O, N) can be estimated using Brown's empirical equation as follows:

$$V = \sum s$$

$$s = \exp[(r_0 - r)/B], \quad B = 0.37$$

The symbol *V* is the oxidation state of atom, and *s* is the bond-valence of the corresponding bond. *r*₀ is the empirical constant, and *r* is bond length. The value *r*₀ was calculated using the equation, *r*₀ = *r*_c + *A* × *r*_a + *P* − *D* − *F*. The *r*_c and *r*_a are contribution to *r*₀ from the cation and anion respectively (these are shown in Table 2 in the ref 9a). The *r*_a for fluorine, nitrogen, and oxygen = −0.11, 0.090, and 0, respectively. The *r*_c for K⁺, Cs⁺, Tl⁺, and La³⁺ = 2.126, 2.438, 2.06, and 2.170, respectively. The *A* value is set to 0.8 for transition metals (groups 3–12) with d electrons; otherwise, it is set to 1.0. *P* = 0.0175 × (cation period − 2), *D* are given in Table 3 in the ref 9a, and *F* = 0.016 × number of f electrons. Here, we calculated each *s* value of F, O, and N.

$$s = \sum s_x, \quad s_x = s(\text{F}\cdots\text{M}^+), \quad s(\text{O}\cdots\text{M}^+), \quad \text{and} \quad s(\text{N}\cdots\text{M}^+)$$

Using this equation, the bond valence values of Tl⁺ **1** and La³⁺ **2** were calculated and are shown in Table 3 along with those of other complexes reported before. Details and examples of the calculation are shown in Supporting Information. The *V* (= ΣΣ_{s_x}) should be equal to the valence of the cation, but in the case of Cs⁺ **2**, the sum of *s* is 1.413 and is larger than 1. This result refers to the size of the cesium ion and the rigidity of the host: the cavity size of **2** does not vary, and thus, when a large cation is included in the cavity, the fluorine–cesium distance is forced to be small.¹¹ Therefore, the value *V* becomes large because the bond-valence, *s*, is a function of distance between the cation and the ligand. In a system where each ligand moves freely, the ligand and cation distance changes, depending on the strength of the bond. However, in the case of the hosts **1** and **2**, in which the position of each ligand is fixed in advance, the value *V* often does not coincide with the valence of the metal

cation. However, we have no trouble in discussing the contribution of each ligand to cation binding. In the case of Tl⁺ **1**, the *s* values are Σ_s(F···Tl) = 0.318 and Σ_s(N···Tl) = 0.087 (*s*(F···Tl) = 0.0530 and *s*(N···Tl) = 0.0218 for each ligand), and thus, the contribution of the fluorine to the cation binding is larger than that of nitrogen. The sum of *s* values (= *V*) is equal to 0.405. Despite the large size of the Tl⁺, the *V* value is much smaller than 1 in contrast to the Cs⁺ **2**. This result can be explained by the unsaturated coordinating state of the Tl⁺ cation: Tl⁺ is shielded by the host skeleton, and solvent molecules or anions cannot coordinate to the metal center. Brown's equation is most effective in the case of salts or minerals in which cations and anions are placed at the most stable site and satisfied coordination number. These conditions are not necessarily satisfied in the case of cage compounds such as **1** and **2** in which coordination numbers and geometries of the cations in the cavities are enforced by the ligands.

In the case of La³⁺ **2**, the *s* values are Σ_s(F···La) = 0.682, Σ_s(O···La) = 0.149, and Σ_s(N···La) = 0.314 (*s*(F···La) = 0.171, *s*(O···La) = 0.0745, and *s*(N···La) = 0.0785 for each ligand), and the contribution of fluorine to the cation binding is larger than that of oxygen or nitrogen. Also here, the *V* value is equal to 1.145 and is much smaller than 3 because La³⁺ has a small ionic radius (1.03 Å) and La³⁺ is unsaturated in the cavity the same as Tl⁺ **1**.¹¹ In the case of cation complexes of **1** and **2**, the position of each donor (C–F, N, and O) is forcibly determined by the structure of the hosts **1** and **2**. Therefore, the C–F···M⁺ distances inevitably become shorter than those of N···M⁺ and O···M⁺, and thus the *s*(F···M⁺) values become large. Accordingly, it is dangerous to conclude directly from bond valence calculations that C–F interacts more strongly than ether oxygen or amine nitrogen. However, as previously reported, the −Δ*H* values of cation inclusion are relatively large, and sometimes the stabilization energy is comparable to that of crown ethers or cryptands.⁵ Therefore, it is a fact that the C–F···M⁺ interaction involves a relatively large attractive force.

Additionally, another remarkable phenomenon is that no water or solvent molecules are coordinated to La³⁺. This is a rare case in the lanthanide complexes. J.-M. Lehn et al. reported lanthanide complexes of their cryptands, but they could not realize the dehydrated complexes.¹² In the case of **1** and **2**, the highly hydrophobic nature of the units which construct the molecular skeleton of the hosts is well recognized by this fact. We previously reported that such an effect of the hydrophobic wall of similar cage compounds greatly influences the complex formation.¹³

NMR Spectroscopic Features. When the C–F unit of **1** and **2** interacts with cations, several NMR spectroscopic features, that is (1) the ¹⁹F NMR signal shifts to higher fields, (2) the coupling constant *J*_{C–F} is reduced, and (3) the benzylic proton signal shifts to lower fields, are observed.^{2–5} Furthermore, a new property, (4) spin coupling, was added in the case of Cs⁺ **1** and **2**: the ¹⁹F NMR spectrum in each complex showed a signal split into an octet (*J*_{Cs–F} = 35.1 Hz for Cs⁺ **1** and 54.9 Hz for Cs⁺ **2**, *I* (¹³³Cs) = 7/2).¹⁴ These are very rare

(12) Bkouche-Waksman, I.; Guilhem, J.; Pascard, C.; Alpha, B.; Deschenaux, R.; Lehn, J.-M. *Helv. Chim. Acta* **1991**, *74*, 1163–1170.

(13) (a) Takemura, H.; Shinmyozu, T.; Inazu, T. *J. Am. Chem. Soc.* **1991**, *113*, 1323–1331. (b) Takemura, H.; Shinmyozu, T.; Inazu, T. *Coord. Chem. Rev.* **1996**, *156*, 183–200. (c) Takemura, H.; Kon, N.; Tani, K.; Takehara, K.; Kimoto, J.; Shinmyozu, T.; Inazu, T. *J. Chem. Soc., Perkin Trans. 1* **1997**, 239–246. (d) Takemura, H.; Inazu, T. *J. Synth. Org. Chem. Jpn.* **1998**, *56*, 604–614.

(14) Takemura, H.; Kon, N.; Kotoku, M.; Nakashima, S.; Otsuka, K.; Yasutake, M.; Shinmyozu, T.; Inazu, T. *J. Org. Chem.* **2001**, *66*, 2778–2783.

(11) We appreciate Professor Emeritus I. D. Brown's kind comments on the interpretations of the results of the calculation.

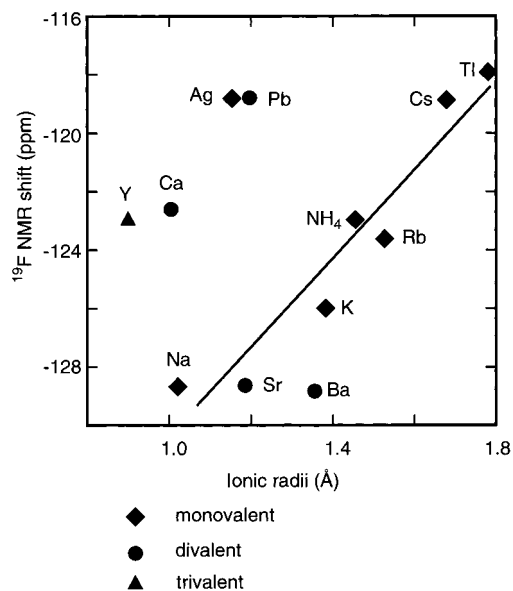


Figure 7. Plots of ^{19}F NMR shift of $\text{M}^{n+} \subset \mathbf{1}$ vs ionic radii.

cases and, only two other examples were reported by Davidson et al., so far.¹⁵ The spin coupling was also observed in the TI^+ complexes of $\mathbf{1}$ and $\mathbf{2}$; namely, the doublets ($J_{\text{TI-F}} = 2914$ Hz for $\text{TI}^+ \subset \mathbf{1}$ and 4558 Hz for $\text{TI}^+ \subset \mathbf{2}$, $I(^{203,205}\text{TI}) = 1/2$) were observed at room temperature. Thus, the C–F···M⁺ interaction can be confirmed visually in these complexes. A coupling ^{19}F – $^{203/205}\text{TI} = 3537$ Hz was reported in a fluorinated complex at low temperatures.¹⁶

Previously, we reported a good linear relationship between ^{19}F NMR shifts and ionic radii in the alkali metal complexes $\text{M}^+ \subset \mathbf{1}$, $\mathbf{2}$.^{5,14} Among the metal cations observed in this study, only TI^+ is on this line, and the relationship does not apply in the case of the complexes of Ca^{2+} , Sr^{2+} , Ba^{2+} , Ag^+ , Pb^{2+} , and Y^{3+} (Figure 7). Contrary to this result, the chemical shifts of the methylene proton $-\text{CH}_2-$ and the ionic radii of the included cations are in good linear relationship, depending on the valences of the metal cations (Figure 8). A plot of the silver cation deviates from the line, and a similar phenomenon was observed in the case of the silver complex of $\mathbf{2}$. However, the reason for this large deviation cannot be explained so far. We also observed the relationship between stability constants and coupling constants $J_{\text{C-F}}$ in the previous report.¹⁴ The relationship between the NMR spectral features (chemical shifts or coupling constants) and the ionic radii of the included cations shows the correlation of the change in electron density between F and M⁺ atoms accompanied by the change in interatomic distances.

Nature of C–F···M⁺ Interaction. The crown ethers trap cations by cation–dipole interaction; on the other hand, a coordination bond is important in the case of polycyclic amines. Thus, a difference in affinity toward alkali metals, alkaline earth metals, and transition metals occurs. The selectivity is not determined only by the soft–hard combination.

Here, the potential energy of the charge Q which is located at a distance of r from a dipole can be expressed by the equation shown in Figure 9. Substituting the data for the $\text{K}^+ \subset \mathbf{1}$ (F···K⁺ distances and C–F···K⁺ angles based on the X-ray crystallographic analysis) in the equation, we can estimate the

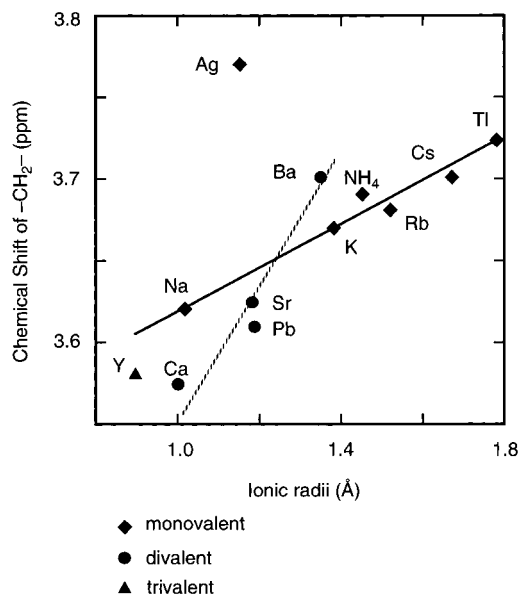


Figure 8. Plots of ^1H NMR shift ($-\text{CH}_2-$) of $\text{M}^{n+} \subset \mathbf{1}$ vs ionic radii.

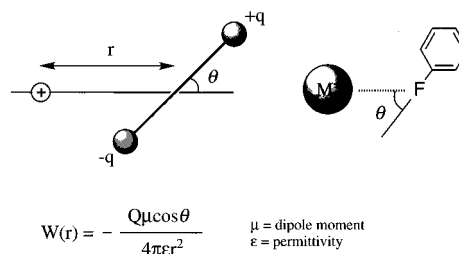


Figure 9. Representation of cation–dipole interaction.

magnitude of the cation–dipole interaction. Consequently, the stabilization energies, 33.7 kcal mol⁻¹ in a vacuum and 6.2 kcal mol⁻¹ in fluorobenzene, were obtained. As previously reported, we measured $-\Delta H = 16.1$ kcal mol⁻¹ of the K⁺ inclusion reaction, and thus, the rough calculation described above reproduces well this observed $-\Delta H$ value.⁵ Accordingly, the major part of the C–F···M⁺ interaction is considered to be cation–dipole interaction. This result explains the fact that compound $\mathbf{1}$ captures soft cations Ag^+ and TI^+ strongly, although $\mathbf{1}$ has a hard donor, fluorine. However, we should note that the interaction is greatly affected by the dielectric constant ϵ of the medium, and it becomes very small in solvents with large ϵ values. For example, in a solvent like water ($\epsilon = 80.1$, 20 °C) or acetonitrile ($\epsilon = 37.5$, 20 °C), the stabilization energy is reduced to 0.36 or 0.76 kcal mol⁻¹, respectively.

On the other hand, coordination ability toward cations is associated with electron-donating ability. Therefore, Kagiya's electron-donating power, $\Delta\nu_{\text{D}}$, was measured and compared in the series of compounds, fluorobenzene, diethyl ether, and triethylamine, which are considered to be equal to the donor units of the compounds $\mathbf{1}$ and $\mathbf{2}$.¹⁷ The results are summarized in Table 4 along with dipole moments of the compounds.¹⁸ As a result, it is revealed that the electron-donating property of fluorobenzene is extremely weak. If the coordination ability is the major power in the C–F···M⁺ interaction, Teflon may absorb metal cations. Nevertheless, we must recognize that there is an electron transfer from the fluorine atom (fluorobenzene unit) to the metal cation (or from the metal to the fluorine atom); namely, a coordination bond is present between C–F and M⁺,

(15) (a) Boyd, A. S. F.; Davidson, J. L.; McIntosh, C. H.; Leverd, P. C.; Lindsell, W. E.; Simpson, N. J. *J. Chem. Soc., Dalton Trans.* **1992**, 2531–2532. (b) Davidson, J. L.; McIntosh, C. H.; Leverd, P. C.; Lindsell, W. E.; Simpson, N. J. *J. Chem. Soc., Dalton Trans.* **1994**, 2423–2429.

(16) Bakar, W. A. W. A.; Davidson, J. L.; Lindsell, W. E.; McCullough, K. J. *J. Chem. Soc., Dalton Trans.* **1990**, 61–71.

(17) Kagiya, T.; Sumida, Y.; Inoue, T. *Bull. Chem. Soc. Jpn.* **1968**, *41*, 767–773.

(18) *Lange's Handbook of Chemistry*; McGraw-Hill: New York, 1985.

Table 4. Dipole Moments μ (D) and Kagiya's Electron-donating Power $\Delta\nu_D$

	μ (D)	$\Delta\nu_D$
fluorobenzene	1.61	-15
diethyl ether	1.15	78
triethylamine	0.77	238

because we can observe clear NMR (^1H , ^{13}C , and ^{19}F) spectroscopic changes (chemical shift or spin coupling).

Conclusions

The C-F \cdots M $^+$ interaction was proved by complexation experiments between host compounds **1**, **2**, and metal cations. The stability of the complexes is determined by the properties of metal cations (ionic radii and ease of hydrolysis), and it is not related to a soft-hard property. By measurement of the electron-donating ability of fluorobenzene, the C-F unit appeared to be a very poor electron donor. A simple calculation shows that the enthalpy change $-\Delta H$ of the cation complexation reaction can be expressed by the cation-dipole interaction. From these results, it was concluded that the cation-dipole interaction is predominant in the C-F \cdots M $^+$ interaction and that the coordination bond operates supplementally. Therefore, all of the cations interact with the C-F unit, and it acts as donor similar to ether oxygen or amine nitrogen. In some cases such as Cs $^+$ and Tl $^+$ complexes, we can observe the interaction via electrons. The spatial arrangement and number of the C-F unit, namely, the preorganization of the donor unit, is important to observe the interaction with sufficient magnitude. We must keep in mind that the C-F \cdots M $^+$ interaction greatly depends on the C-F \cdots M $^+$ angle and the polarity of the solvent because the cation-dipole interaction is a major factor in it.

Experimental Section

General Procedure. The ^1H , ^{13}C , and ^{19}F NMR spectra were respectively recorded at 400.1, 100.6, and 376.5 MHz, with TMS and CFCl_3 as internal references. FAB mass spectra were obtained with *m*-NBA as a matrix. Elemental analyses were performed at the Service Centre of the Elementary Analysis of Organic Compounds affiliated with the Faculty of Science, Kyushu University. All solvents and reagents were of reagent quality and were used without further purification.

Measurements of $\Delta\nu_D$: Donor Ability of the Solvents. The measurements were performed according to a literature method.¹⁷ The IR spectra were recorded with a NaCl cell (0.2 mm) at 30 °C. Methyl alcohol-*d* (CH_3OD) was dissolved in benzene, fluorobenzene, diethyl ether, and triethylamine at a concentration of ca. 0.2 mol dm^{-3} . The $\Delta\nu_D$ values thus obtained were identical to that of the literature within experimental error.

Tl $^+$ \subset **1·NO $_3^-$.** A mixture of **1** (31.0 mg, 3.9×10^{-2} mmol), TlNO $_3$ (14.5 mg, 5.4×10^{-2} mmol), 9 mL of CH_3CN , and 1 mL of water was heated under reflux for 2 days. After removal of the solvent, the residue was recrystallized from CH_2Cl_2 - CH_3CN (colorless granules, 25.0 mg, 60.3%): mp > 261.7 °C (dec in a N $_2$ sealed tube); ^1H NMR (400.1 MHz, $\text{CDCl}_3/\text{CD}_3\text{CN} = 1/1$, v/v, TMS) $\delta = 7.31$ (s, 12H, ArH), 7.07 (t, $J = 7.5$ Hz, 6H, ArH), 3.72 (s, 24H, $-\text{CH}_2-$); ^{13}C NMR (100.6 MHz, $\text{CDCl}_3/\text{CD}_3\text{CN} = 1/1$, v/v, TMS) $\delta = 159.5$, 157.8 (d, $^1J_{\text{C-F}} = 247.0$ Hz), 132.1, 131.8, 131.6, 131.3, 131.0 (quint, $J = 43$ Hz), 125.5 (s), 124.0, 123.7, 123.3, 123.1, 122.8 (quint, $J = 43$ Hz), 54.6 (s); ^{13}C NMR (off-resonance) $\delta = 159.9$ (s), 157.4 (s), 131.6 (dd, $J = 161$ Hz, 8 Hz), 125.5 (s), 123.4 (d, $J = 162$ Hz), 54.5 (t, $J = 135$ Hz); ^{19}F NMR (564.7 MHz, $\text{CDCl}_3/\text{CD}_3\text{CN} = 1/1$, v/v, CFCl_3) $\delta = -114.01$, -121.75 (d, $^1J_{\text{F-Tl}} = 2914$ Hz). MS (FAB): m/z (%) 991 (16.4) [$\text{M} + ^{203}\text{Tl}^+$], 993 (34.3) [$\text{M} + ^{205}\text{Tl}^+$]. Anal. Calcd for $\text{C}_{48}\text{H}_{42}\text{N}_6\text{F}_6 \cdot \text{TlNO}_3$: C, 54.63; H, 4.01; N, 6.64. Found: C, 54.64; H, 4.05; N, 6.63.

La $^{3+}$ \subset **2·(CF $_3$ SO $_3^-$) $_3$.** A mixture of **2** (30.0 mg, 3.9×10^{-2} mmol), La(CF $_3$ SO $_3$) $_3$, (65.5 mg, 11.2×10^{-2} mmol), 5 mL of CHCl_3 , and 5 mL of CH_3CN was heated under reflux for 1 day. After removal of the solvent, the residue was recrystallized from CH_2Cl_2 - CH_3OH . The resultant colorless granules (37.2 mg) were a mixture of $2\text{H}^+ \subset 2 \cdot (\text{CF}_3\text{SO}_3^-)_2$ and $\text{La}^{3+} \subset 2 \cdot (\text{CF}_3\text{SO}_3^-)_3$.

X-ray Crystallographic Data. Crystal data for $\text{Tl}^+ \subset 1 \cdot \text{NO}_3^-$: $\text{C}_{54}\text{H}_{42}\text{N}_6\text{F}_6\text{TlO}_3$, $M_r = 1169.34$ g mol^{-1} , colorless needles (grown from CH_2Cl_2 - CH_3CN mixture), size 0.50 mm \times 0.10 mm \times 0.50 mm, monoclinic, space group $P2_1/n$ (No. 14), $a = 15.1647(6)$ Å, $b = 21.9735(9)$ Å, $c = 14.9533(6)$ Å, $\beta = 90.822(1)^\circ$, $V = 4982.2(4)$ Å 3 , $Z = 4$, $\rho_{\text{calcd.}} = 1.559$ g cm^{-3} , $\mu(\text{Mo K}\alpha) = 33.12$ cm^{-1} , $F(000) = 2324.00$, $T = -180 \pm 1$ °C using the $\omega - 2\theta$ scan technique to a maximum 2θ value of 55.0°. A total of 43461 reflections were collected. The final cycle of the full-matrix least-squares refinement was based on 6880 observed reflections ($I > 2.00\sigma(I)$) and 748 variable parameters and converged with unweighted and weighted agreement factors of $R = 0.065$, $R_w = 0.216$, and GOF = 1.01. The maximum and minimum peaks on the final difference Fourier map corresponded to 0.87 and -2.34 e $^-/\text{Å}^3$, respectively.

Crystal data for $[\text{La}^{3+} \subset 2 \cdot (\text{CF}_3\text{SO}_3^-)_3]_{0.15} \cdot [2\text{H}^+ \subset 2 \cdot (\text{CF}_3\text{SO}_3^-)_2]_{0.85}$: $\text{C}_{43}\text{H}_{44}\text{N}_4\text{O}_9\text{F}_{10}\text{S}_2\text{La}_{0.15}$, $M_r = 1035.78$ g mol^{-1} , colorless platelet crystal (grown from CH_2Cl_2 -MeOH mixture), size 0.50 mm \times 0.05 mm \times 0.50 mm, triclinic, space group $P\bar{1}$ (No. 2), $a = 13.756(1)$ Å, $b = 15.318(1)$ Å, $c = 13.747(1)$ Å, $\alpha = 116.106(2)^\circ$, $\beta = 112.830(3)^\circ$, $\gamma = 89.667^\circ$, $V = 2349.4(3)$ Å 3 , $Z = 2$, $\rho_{\text{calcd.}} = 1.46$ g cm^{-3} , $\mu(\text{Mo K}\alpha) = 3.4$ cm^{-1} , $F(000) = 1065.10$, $T = -180 \pm 1$ °C using the $\omega - 2\theta$ scan technique to a maximum 2θ value of 55.0°. A total of 16555 reflections were collected. The final cycle of the full-matrix least-squares refinement was based on 6764 observed reflections ($I > 2\sigma(I)$) and 667 variable parameters and converged with unweighted and weighted agreement factors of $R = 0.080$, $R_w = 0.262$, and GOF = 1.05. The maximum and minimum peaks on the final difference Fourier map corresponded to 0.75 and -0.59 e $^-/\text{Å}^3$, respectively. The crystal structure was measured and determined as a mixture of two components. The composition of the two components was determined using the SHELXL-97 program.¹⁹

Crystallographic data (excluding structure factor) for structures reported in this paper have been deposited with the Cambridge Crystallographic Data Centre as supplementary publication no. CCDC-161196 for $\text{Tl}^+ \subset 1$, and no. CCDC-161195 for $\text{La}^{3+} \subset 2$. Copies of the data can be obtained free of charge on application to CCDC, 12 Union Road, Cambridge CB21EZ, UK (fax: (+44)1223-33603; e-mail: deposit@ccdc.cam.ac.uk).

Acknowledgment. This research was supported by a Grant-in-Aid for Developmental Scientific Research provided by the Ministry of Education, Science, Sports and Culture, Japan (No. 12640522), and for COE Research "Design and Control of Advanced Molecular Assembly Systems" from the Ministry of Education, Science, Sports and Culture, Japan (No. 08CE2005). We thank Professor Emeritus I. D. Brown for his kind comments on the discussion of bond valence sum.

Supporting Information Available: Calculation method of Brown's bond valence, molecular structure of $2\text{H}^+ \subset 2 \cdot (\text{CF}_3\text{SO}_3^-)_2$ and $\text{Tl}^+ \subset 1 \cdot \text{NO}_3^-$ (pentacoordinated). X-ray crystallographic data of $\text{Tl}^+ \subset 1 \cdot \text{NO}_3^-$ and $[\text{La}^{3+} \subset 2 \cdot (\text{CF}_3\text{SO}_3^-)_3]_{0.15} \cdot [2\text{H}^+ \subset 2 \cdot (\text{CF}_3\text{SO}_3^-)_2]_{0.85}$. This material is available free of charge via the Internet at <http://pubs.acs.org>. See any current masthead page for ordering information and Web access instructions.

JA0043587

(19) Sheldrick, G. M. A program for the refinement of crystal structures. University of Goettingen: Germany, 1997.